




Review

Overview of Theory, Simulation, and Experiment of the Water Exit Problem

Hualin Zheng ¹, Hongfu Qiang ¹, Yujie Zhu ^{1,*} and Chi Zhang ^{2,3}

¹ Xi'an Research Institute of Hi-Tech, Xi'an 710025, China; zero2one@aliyun.com (H.Z.)

² TUM School of Engineering and Design, Technical University of Munich, 85748 Garching, Germany

³ Huawei Technologies Munich Research Center, 80992 Munich, Germany

* Correspondence: yujie.zhu@tum.de

Abstract: The water exit problem, which is ubiquitous in ocean engineering, is a significant research topics in the interaction between navigators and water. The study of the water exit problem can help to improve the structural design of marine ships and underwater weapons, allowing for better strength and movement status. However, the water exit problem involves complex processes such as three-phase gas–liquid–solid coupling, cavitation, water separation, liquid surface deformation, and fragmentation, making it challenging to study. Following work carried out by many researchers on this issue, we summarize recent developments from three aspects: theoretical research, numerical simulation, and experimental results. In theoretical research, the improved von Karman model and linearized water exit model are introduced. Several classical experimental devices, data acquisition means, and cavitation approaches are introduced in the context of experimental development. Three numerical simulation methods, namely, the BEM (Boundary Element Method), VOF (Volume of Fluid), and FVM (Finite Volume Method) with LES (Large Eddy Simulation) are presented, and the respective limitations and shortcomings of these three aspects are analyzed. Finally, an outlook on future research improvements and developments of the water exit problem is provided.

Keywords: water exit; theoretical research; numerical simulation; experimental development; cavitation



Citation: Zheng, H.; Qiang, H.; Zhu, Y.; Zhang, C. Overview of Theory, Simulation, and Experiment of the Water Exit Problem. *J. Mar. Sci. Eng.* **2024**, *12*, 1764. <https://doi.org/10.3390/jmse12101764>

Academic Editor: Dejan Brkić

Received: 21 August 2024

Revised: 20 September 2024

Accepted: 25 September 2024

Published: 5 October 2024



Copyright: © 2024 by the authors. Licensee MDPI, Basel, Switzerland. This article is an open access article distributed under the terms and conditions of the Creative Commons Attribution (CC BY) license (<https://creativecommons.org/licenses/by/4.0/>).

1. Introduction

The development of technology and manufacturing ability has enabled us to cross the gap of the ocean and explore the unknown world. However, the complex phenomena and mechanisms of interaction between navigators and water are ubiquitous in ocean engineering, and are of great significance to the study these problems in regard to structural safety, transportation efficiency, and target deployment [1–5]. In 1929, von Karman, in his pioneering study the seaplane water entry impact problem, conducted theoretical and experimental research on the interaction between navigators and water [6]. Wagner (1932) [7] expanded on von Karman's theory, specifically by further investigating the free surface deformation during the water exit of two-dimensional bodies. These studies on water exit problems mainly served in the design of seaplanes, ships, bridges and offshore platforms [8], helping engineers to better predict the stress situation of structures in water. Since then, numerous researchers have deepened the exploration of this issue through theoretical analysis, experimental research, and numerical simulations, achieving significant outcomes that have propelled the design and manufacturing of ships, underwater vehicles, and seaplanes [9–16].

According to the manner of structures crossing the water interface, interactions between the navigators and water may include water entry, in-water motion, and water exit processes. Among these, study of the water entry and water exit stages is complicated by their multi-phase and cross-media nature. Water entry scenarios, which are widely present in ocean engineering [17–20], AUVs (Autonomous underwater vehicles) engineering [21–23], and natural phenomena [24–26], have attracted much attention and extensive research. In the early stage of

water entry study, flow visualization via high-speed camera [27–29] was applied to capture the details of flow. Subsequently, many experimental [30,31] and numerical [32,33] studies have been carried out to analyze pressure distribution, impact force, shape design, and cavitation.

However, compared to the water entry problem, much less work has been conducted on the water exit problem. This is due to the fact that the physical processes and nonlinear properties involved in the water exit problem are much more complex than those of the water entry problem. Although both the water entry and water exit problems involve interactions between a solid object and fluid surface, they present distinct differences in their physical characteristics. In the course of water entry, the object experiences increasing drag as it penetrates the water surface, leading to surface deformation, splashing, and bubble formation. Added mass effects increase as the object moves deeper into the water. In contrast, during water exit the object encounters decreasing drag as it leaves the water, and phenomena such as cavitation and wake formation are prominent. Both processes involve fluid separation and surface dynamics, which are critical in marine structural design. These characteristics play an essential role in applications such as floating platforms and underwater vehicles, where understanding surface behavior helps to optimize performance. Although water exit and water entry appear to be opposite physical processes, the water exit problem cannot simply be treated as the reverse of the water entry problem. Oliver [34] provides specific explanations in the context of the stability of theoretical solutions according to the implicit dispersion relation obtained by matching the water entry and water exit solutions. Insights into the stability of theoretical solutions indicate that the leading-order water exit problem is only linearly stable when the turnover curve is increasing, suggesting that water exit phenomena cannot be considered as merely the reverse of water entry. In addition, Ni et al. [35] found that, contrary to the gradual increase of fluid load and fluid–solid coupling force during water entry, water exit is a process with a reducing wetted area, gradual solid–liquid separation, and smaller fluid load. Furthermore, it is more challenging to apply Wagner’s theory [36], which utilizes a linear free-variable interface condition with a correction for the water line.

Although the water exit problem is very complex, and involves multiphase flows, phase changes, turbulence, and cavitation or super-cavitation, it has a wide range of applications as well, including drag reduction [1], underwater navigation [37], unmanned aerial–underwater vehicles [38,39], and more, which have attracted great attention in many fields [1,4,40–42]. In the early stages, exploration of water exit mainly focused on analytic research [6,7]. With advances in experimental setup and numerical technology, scholars have gradually begun to verify the accuracy of theoretical models through experiments and numerical simulations. Greenhow (1983, 1987, 1997) [43–45] conducted a series of experimental studies on the phenomena of free surface rupture and water flow separation during the process of cylindrical outflow. Miao’s experiments (1988) [46] on water exit using horizontal cylinder showed the significance of surface tension and cavitation in reducing the additional mass force. Their experimental data provided support for the design of marine structures and helped to improve their resistance to wind and waves in complex marine environments. Ye et al. (1990) [47] used a perturbation method based on small angles to study the problem of object tilting out of water. A set of axisymmetric two-dimensional equations were used to approximate the three-dimensional equations, and the BEM (Boundary Element Method) was used to solve the process before the object approached the free liquid surface. Zhang et al. (2015, 2018) [48,49] conducted water exit experiments of axisymmetric objects and low-density floating bodies, and additionally investigated the deformation of a free surface, including the rupture and separation of the object. Yang (2023) [50] and Yun (2024) et al. [51,52] respectively investigated the water exit problem of cylinders by experiments and SPH (Smoothed Particle Hydrodynamics), demonstrating the characteristics of impacting force and hydrodynamic response of the structures in the process. These studies provided valuable data support for the design optimization of floating platforms and underwater detection equipment, which can better serve

practical applications in ocean engineering, especially design issues related to breakwaters and floating platforms.

In contemporary society, growing demand in civilian sectors such as ocean resource development, maritime transportation, and environmental monitoring has underscored the increasing significance of research on water discharge phenomena [53,54]. For instance, in the construction of offshore wind farms, the inflow and outflow around wind turbine foundations in tidal environments have a direct impact on the safety and lifespan of the structures. Similarly, offshore oil and gas extraction platforms must account for water effects in order to maintain stability in complex marine conditions. In the field of environmental monitoring, automated devices such as AUVs [55] frequently traverse the water surface for data collection and transmission. Understanding the aerodynamic and hydrodynamic forces during water discharge is essential for optimizing design and ensuring operational stability of these devices across varied environmental conditions. The present work summarizes studies on the water exit problem conducted by researchers since von Karman, including theoretical research, numerical simulation, and experimental development. Current developments and difficulties in research on the water exit problem are summarized and analyzed, and possible future research directions are provided.

The rest of this paper is organized as follows: Section 2 presents two kinds of theories in detail to describe the water exit process; Section 3 summarizes the water exit experiments conducted in previous research; Section 4 presents several numerical simulation methods for solving the water exit process; finally, Section 5 concludes with a discussion of the current development of the water exit problem and provides several outlooks on future research.

2. Theoretical Research

Due to the problem's complex nonlinear property, theoretical research on water exit phenomena remains insufficient. Although many studies have been conducted, including line source distributions and slender body theory [56–58], linear theory [43,59], and added-mass theory [60–62], all of these theories face many limitations in practical applications and provide unsatisfactory prediction accuracy. This section presents two theoretical water exit models, namely, the improved von Karman model and the linearized water exit model. The improved von Karman model originates from the von Karman model [6], which has been successfully adopted to calculate the hydrodynamic forces acting on a seaplane landing on water. The linearized water exit model is mainly used to calculate the hydrodynamic forces acting on the object during the water exit of a rigid body with constant acceleration.

2.1. Improved von Karman Model

The von Karman model, first proposed to solve the hydrodynamic forces during a seaplane landing, agrees well with experimental data [6] but cannot be applied to the water exit process directly due to the discontinuity of the physical quantities at the contact points in the water entry–exit process. To address this issue, Tassin [63] proposed the improved von Karman model for the water exit problem, which is achieved by approximating the derivative of the object's potential function based on the acceleration potential function and its Taylor expansion.

To maintain the continuity of the contact point coordinates in the water entry–exit process, the reference level is modified; furthermore, to guarantee pressure continuity in the water entry–exit process, the derivative of the object potential function is approximated based on the acceleration potential function and its Taylor expansion. Thus, the force in the vertical direction of the object is obtained as follows:

$$F(t) = -\rho \int_{-c(t)}^{c(t)} \left[Zb(y, t) \cdot Zb_{tt}(y, t) + \frac{I_4(y, t)}{\pi} \sqrt{c^2(t) - y^2} \right] dy \quad (1)$$

where $I_4(y, t) = PV \int_0^{c(t)} \frac{-2\tau\theta_i(\tau, t)}{(\tau^2 - y^2)\sqrt{c^2(t) - \tau^2}} d\tau$, $Zb(y, t)$ represents the shape function of the object, $c(t)$ is the contact point position, PV denotes a principal value integral and can be set as a constant, and $\theta_i(y, t)$ is the stream function on the body's surface.

The water entry–exit process of a two-dimensional rigid wedge was simulated by Piro in [64]. In this model, the initial velocity is set as $V_0 = 4 \text{ ms}^{-1}$, the angle of attack $\beta = 10^\circ$, and the acceleration $a = 92 \text{ ms}^{-2}$. The displacement equation is $h(t) = Vt - \frac{1}{2}at^2$; when $t_0 = V_0/a$, the velocity V decreases to 0 ms^{-1} , where t_0 is set as the dimensionless time reference variant with the dimensionless time $t^* = t/t_0 = at/V_0$. Therefore, when $0 < t^* < 1$, the object is in the water entry stage, and the theoretical force can be obtained by Wagner's theory [7,36]. When $t^* > 1$, the object is in the water exit stage and the theoretical force can be solved by the linearized model. Using $F_{sc} = \rho(V/2)^2 B$ as the dimensionless force reference variant, the dimensionless force is $F^*(t^*) = F(t)/F_{sc}$. The force evolution during the water entry and exit of a wedge obtained by this model is shown in Figure 1.

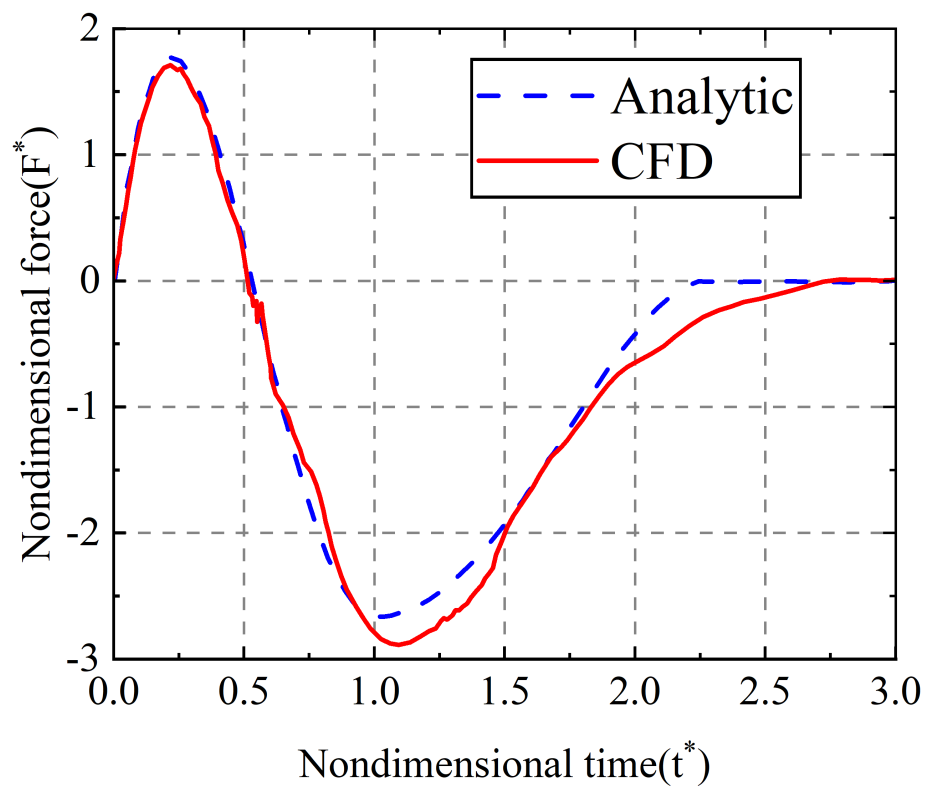


Figure 1. Force evolution during the water entry and exit of a wedge. Reproduced from [63] with permission from Elsevier/2024.

Adel Shams [65] described the water exit process of the wedge with the improved von Karman model and obtained pressure field data from water entry to water exit via PIV (Particle Image Velocimetry) technology (see [65]), which were in good agreement.

2.2. Linearized Water Exit Model

The linearized water exit model was proposed in [66]. It is only applicable to symmetric rigid bodies initially located at the free liquid surface with uniform acceleration water exit vertically. Based on the assumption that the velocity at the contact point is proportional to that of the local fluid, then linearizing the pressure, this model was developed without taking into account the shape of the object, and good agreement with numerical simulation was achieved [66]. In order to solve water exit problem with changing acceleration, the model was further modified by taking into account the object shape and some nonlinear terms in Bernoulli's equation [63]. This research improved the theoretical

prediction accuracy, and was applied to investigate the steady-state problem of ellipsoidal bodies moving along the water surface in a shallow submerged state.

The linearized water exit model can be linearized according to the following:

(1) The time range of the water exit phase is $0 < t < T$, in which the vertical displacement of the object is of order $O(aT^2)$. The order of vertical displacement is much smaller than the reference dimension, i.e., aT^2/c_0 , which is far less than 1. For the reference dimension aT^2/c_0 , c_0 denotes the reference dimension for length and object acceleration a as the reference dimension for flow acceleration.

(2) The fluid velocity $v(x, t)$ is of order $O(aT)$.

(3) The viscous term $v\nabla^2v$ in the NS equation can be neglected because $\frac{|v\nabla^2v|}{|v_t|} = O(vT/c_0^2)$, and in the early stage of water exit $vT/c_0^2 \ll 1$ ($v \approx 1.004 \times 10^{-6} \text{ m}^2\text{s}^{-1}$ at 20 °C). The convective term $(v \cdot \nabla)v$ can be ignored because $\frac{|(v \cdot \nabla)v|}{|v_t|} = O(aT^2/c_0) \ll 1$. These two approximations are valid in the main flow region and can be ignored; however, the approximation is no longer satisfied in the flow region close to the object, where submergence depth, fluid viscosity, and contact line motion properties all have significant influence.

(4) When the acceleration a is large, $g/a \ll 1$; thus, the gravity can be neglected.

(5) The extension velocity $\frac{dc}{dt}$ of the contact point is proportional to the corresponding local fluid velocity, that is $\frac{dc}{dt} = \gamma\varphi_x(c(t), 0, t)$.

The force $F(t)$ acting on the object at moment t can be expressed as

$$F(t) = \int_{-c(t)}^{c(t)} p(x, 0, t)dx = \int_{-c(t)}^{c(t)} -\rho\varphi_t(x, 0, t)dx. \tag{2}$$

From the boundary conditions, we obtain

$$p(x, 0, t) = -h''(t)\sqrt{c^2(t) - x^2} \quad (|x| < c(t)), \tag{3}$$

$$F(t) = \int_{-c(t)}^{c(t)} p(x, 0, t)dx = -0.5\pi\rho c^2(t)h''(t), \tag{4}$$

where $c(t)$ denotes the contact point and $h''(t)$ denotes the object's acceleration.

The numerical calculations based on the open-source finite-volume CFD library OpenFOAMs performed by Piro et al. [67] were compared with the theoretical solutions (Figure 2). The wedge rigid body model is described in Section 2.1.

The water entry–exit problem for a parabolic shape object was simulated by Tassin [63]. In the model, the contour function is set as $y = x^2/(2R)$ ($R = 1.37 \text{ m}$), $V = 1 \text{ ms}^{-1}$, $a = 19.5376 \text{ ms}^{-2}$. The numerical and theoretical solutions are shown in Figure 3.

From Figures 2 and 3, it can be observed that the numerical solution of the water exit stage agrees well with the theoretical solution of the linearized model.

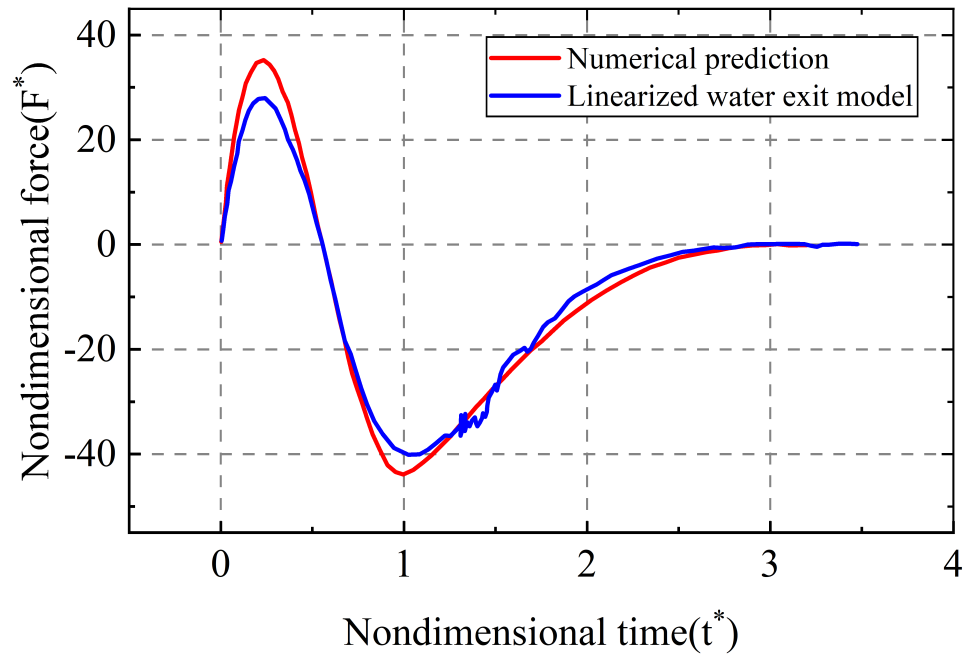


Figure 2. F^* acting on the wedge with respect to t^* . The red line corresponds to the numerical prediction and the blue line to the present model of water exit (where $t^* > 1$) and the Wagner model (where $0 < t^* < 1$). Reproduced from [66] with permission from Cambridge University Press/2024.

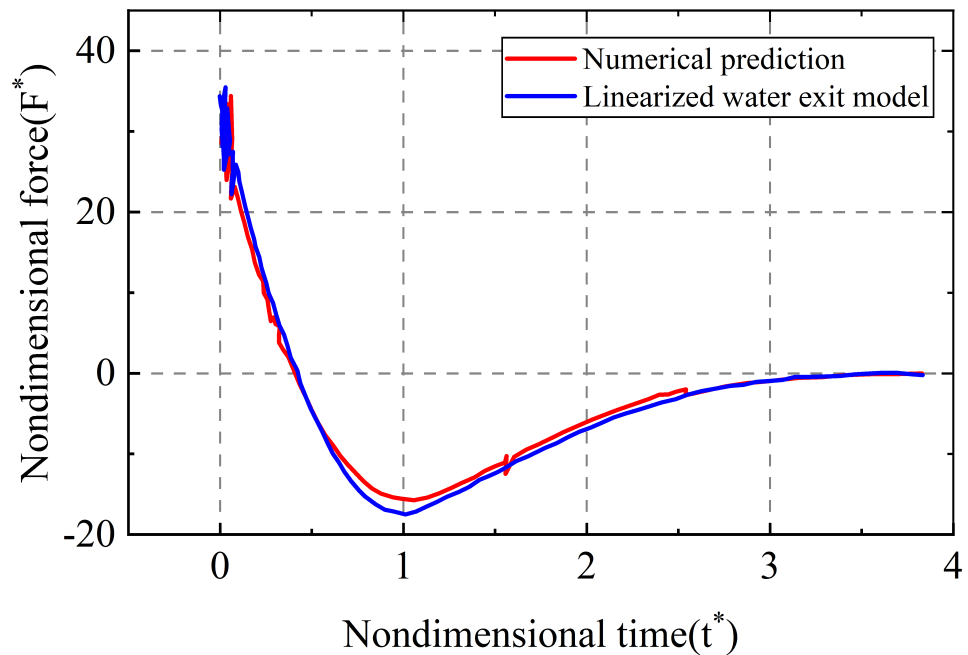


Figure 3. F^* acting on the parabolic with respect to t^* . The red line corresponds to the numerical prediction and the blue line to the present model of water exit (where $t^* > 1$) and the Wagner model (where $0 < t^* < 1$). Reproduced from [66] with permission from Cambridge University Press/2024.

2.3. Discussion

Although the improved von Karman model and linearized water exit model both agree well with numerical results, they are both derived on the basis of several assumptions, as mentioned; thus, there remain some limitations in the following aspects. First, the object models are two-dimensional, and both are rigid bodies. Second, the water exit process is not a pure water exit process, only one stage of the whole water entry–exit process, which can be classified as the semi-submerged water exit process at low speed. Third, the force load of

the object in the vertical direction during the water exit process is deduced in the improved von Karman model, in which it can be seen that the force load is significantly dependent on the position of the contact point $c(t)$. In the water entry process stage, Wagner’s theory can be well applied to evaluate $c(t)$. However, despite some modification, the water separation in the water exit process leads to bias in the calculation. Fourth, for the linearized water exit model, assumptions (1)–(5) are not valid when the penetration depth or velocity increases and the acceleration decreases. The effects of surface tension and viscosity near the water contact area on the surface pressure of the object should be taken into account under those circumstance. Lastly, the nonlinear terms are ignored in both models when calculating the pressure, which is problematic when calculating the impacting force. The linear Bernoulli equation is used in the improved von Karman model, while the linear Euler equation is applied in the linearized water exit model. With increasing structure speed and size, the impact of the nonlinear term on the pressure can no longer be ignored. Tassin et al. also inferred that the nonlinear term would have a remarkable impact on the pressure in the wake region during the water exit process [63]. The advantages and disadvantages of the improved von Karman model and linearized water exit model are summarized in Table 1.

Table 1. Comparison of the improved von Karman model and linearized water exit model.

	Advantages	Disadvantages
Improved von Karman Model	<ol style="list-style-type: none"> 1. Accounts for object shape, improving accuracy in complex geometries. 2. Better handling of both water entry and exit processes. 3. Provides good agreement with experimental data for wedges and PIV data. 	<ol style="list-style-type: none"> 1. Complex to implement due to nonlinear effects and shape considerations. 2. Accuracy decreases for highly irregular objects. 3. Requires Taylor expansion and modifications to maintain continuity.
Linearized Water Exit Model	<ol style="list-style-type: none"> 1. Simplified model, easier to implement for symmetric objects. 2. Provides good agreement with numerical simulations for uniform acceleration cases. 3. High accuracy in early stages of water exit. 	<ol style="list-style-type: none"> 1. Limited to symmetric rigid bodies and constant vertical acceleration. 2. Does not account for gravity in high acceleration cases. 3. Simplifies object shape considerations, which may reduce accuracy in complex cases.

Although there still exist some limitations for the improved von Karman model and linearized water exit model, their exploration in water exit problems provides us with valuable references. On the basis of these two models, there are several aspects worth optimizing and researching more deeply:

(1) From the derivation of the theoretical model, it can be seen that the calculation of the pressure term is the key to solving the hydrodynamic force load. In these two theoretical models, the pressure term is calculated by directly omitting the nonlinear term; thus, it is possible to further explore the linearization of the nonlinear term instead of omitting it to solve the pressure term.

(2) The research object can be expanded from a two-dimensional rigid body to a three-dimensional body, bringing it closer to the actual situation. The current theoretical models are mainly aimed at solving the overall force load on the object during the water exit process. In the actual scenario, most navigation bodies are made of shells, including ships, submarines, missiles, etc. In further research, the influence of the hydrodynamic load on the structural deformation of local navigation bodies could be analyzed in combination with shell structure theory and elastic body theory.

(3) It is possible to expand the research process. The water exit process mentioned above is only one stage of the whole water entry–exit process. The pure fully-submerged water exit process at different depths is worthy of further in-depth study. With increasing exit speed, more complex phenomena such as multiphase flows, cavitation, etc., begin to

emerge. The occurrence of these phenomena and their impact on the navigation body is worthy of further theoretical analysis.

3. Experiment Development

Experiments are the most direct way to obtain first-hand data. However, experiments on water exit processes face many difficulties in practice. The first difficulty lies in the method powering exit velocity underwater. Currently, there are two main approaches, i.e., the active and the forced water exits. Active water exit, such as automatic water exit of the neutral object due to its own buoyancy [44,68–72], use of an air pump to eject objects [63,73–79], etc., has the disadvantages of low exit velocity and interference from the air in the water exit process. In a forced water exit, such as an object exiting the water driven by a thin rope [44,46,63], long rod [80], L-shaped rod [80], or lifting platform [81–83], the components tied to the object cause interference with the fluid field. The second difficulty is the manner of obtaining experimental images. In the underwater stage, bubbles and fine flow structures make it challenging to capture the fluid field in detail when the objects are moving at low speed. If the structure exits at high speed, then the fluid fields around the structure evolve violently, blocking the light of the object image and preventing acquisition of a usable picture. The third difficulty lies in monitoring the experimental data. The velocity displacement and other motion parameters of the structure can be obtained directly via high-speed camera; however, the fluid field, especially the pressure field and velocity field around the object, is not easy to observe. There are two widely-used approaches for this: PIV technology [65,68] and pressure sensors attached to the object [68]. Nevertheless, the local impact force loaded on the moving object and the changes in the internal structural stress are still unavailable via experiment. Lastly, the cost of water exit experiments is far higher than that of water entry experiments, especially for the design of underwater devices.

Despite the difficulties in conducting water exit experiments, many scholars have done a great deal of pioneering research on the water exit problem and obtained many valuable results which have greatly contributed to the verification and development of water exit theory and the design and development of underwater navigation bodies. This section reviews the forced and active water exit experiments conducted by scholars. Furthermore, as cavitation occurs in many experiments under certain conditions, the corresponding research is also summarized at the end of the section.

3.1. Forced Water Exits

In 1983, Greenhow et al. [44] conducted a series of experiments on the water exit process of a neutrally buoyant cylinder initially located at the bottom of a water tank by applying a constant force equal to its gravity through a thin rope, effectively capturing the liquid surface lifting and the liquid surface-breaking phenomena. It was found that liquid surface-breaking could be caused by the interaction between the eddy dislodged from the cylinder and the free liquid surface. The liquid surface deformation due to the rise of the sphere was studied by Lighthill [84], while the forces during the rise of the sphere can be found in the work by Faltinsen [85]. The causes of liquid surface-breaking were also successively studied by Peregrine [86] and Broeck [87]. According to Peregrine's study, a force limit exists for vorticity, otherwise the flow is unstable. Vanden's study further showed that the force on the eddy in Peregrine's corollary is always divergent and will eventually exceed the force limit, leading to the inevitable breakup of the liquid surface.

In his doctoral thesis [46], Miao conducted water exit experiments on horizontal cylinders with 0.512 m/s and 0.764 m/s uniform velocity and obtained the impact coefficient variation curve with time. He stated that the water exit fluid at the upper end of the cylinder makes the additional mass change more smoothly. In addition, when the exit displacement is up to the radius length, the fluid below the cylinder is rapidly filled with a large number of bubbles, which will either create cavities or lead to spontaneous breaking

of the free liquid surface. He also found that surface tension and cavitation may have an important effect in reducing the additional mass force.

Although it is operationally easy to conduct experiments by tying a thin rope to the front section of an object so as to push it to exit, this inevitably disturbs the free liquid surface before water exit. In order to avoid the disturbance, Wu et al. [49,80] used an L-shaped restraint mechanism in their experimental setup, as shown in Figures 4 and 5. Motion control of the object is achieved by electromagnetic force.



Figure 4. Experimental setup in free water exit of a fully submerged object. Reproduced from [49] with permission from Elsevier/2024.

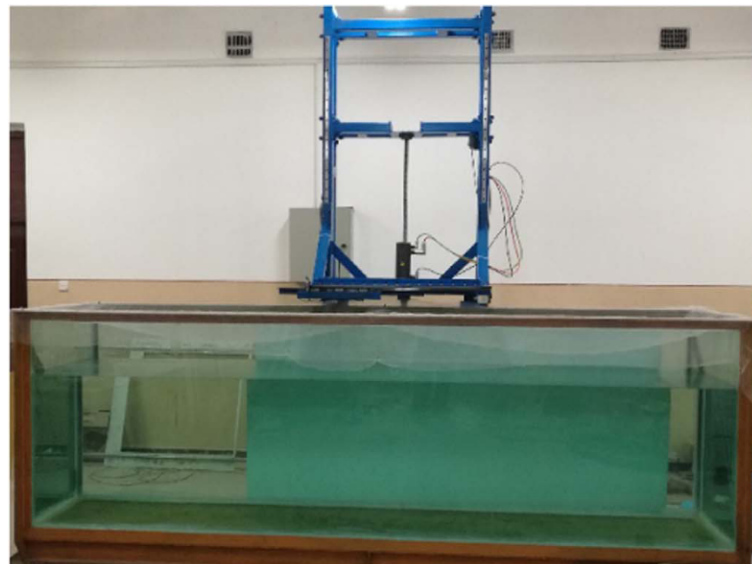


Figure 5. L-shaped restraint mechanism from the experimental setup in Figure 5. Reproduced from [80] with permission from Elsevier/2024.

Using this experimental setup, Wu [80] conducted experiments on fully submerged and partially submerged spheres forced to constantly undergo water exit (0.2–0.7 m/s) (Figure 6), as well as free water exit experiments using a light sphere (density 100 kg/m^3). The effects of different velocities, submersion depths, and Froude numbers on the water exit process were investigated in [80], and the velocity, displacement, acceleration, and drag

coefficient curves with time were also obtained. Furthermore, experiments were conducted on the free water exit and water re-entry process of a hollow light aluminum ellipsoid in [49]. The effects of the relative density (ratio of mass to actual volume) and immersion depth on the water exit process were investigated and the velocity variation curves were obtained, which were in good agreement with the BEM numerical simulation results.

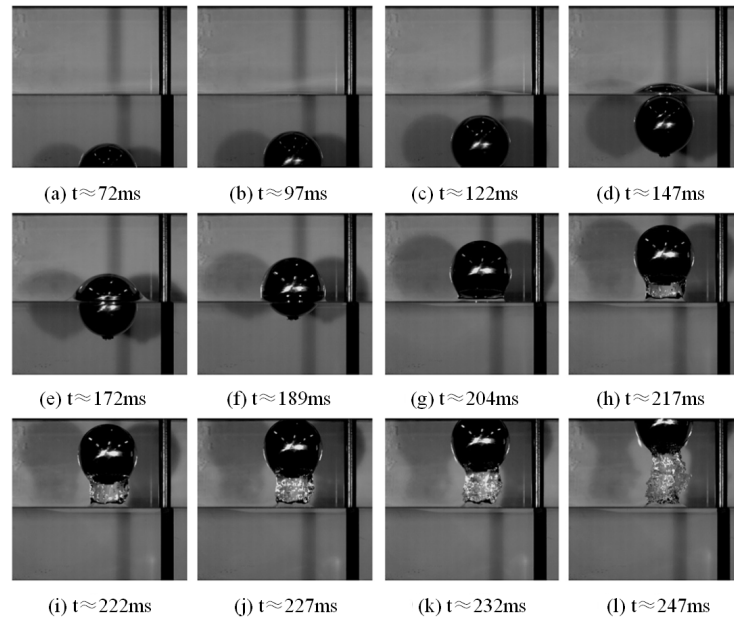


Figure 6. Snapshots of free water exit of a light sphere by Wu. Reproduced from [80] with permission from Elsevier/2024.

Previous water exit experiments mainly focused on the physical parameters of the object itself; the data of the flow field was rarely analyzed, as these data were very difficult to acquire. To address this issue, Adel Shams [65] adopted PIV technology to estimate the fluid velocity field. Experiments were conducted on a specially designed lift tower apparatus (shown in Figure 7) for the whole process of water entry to water exit by a wedge. After obtaining the velocity field, the fluid pressure field was deduced according to the incompressible NS equation. The experimental results showed that, unlike the positive pressure field in the water entry process (with respect to the atmospheric pressure), a negative pressure field occurs in the water exit process [65].

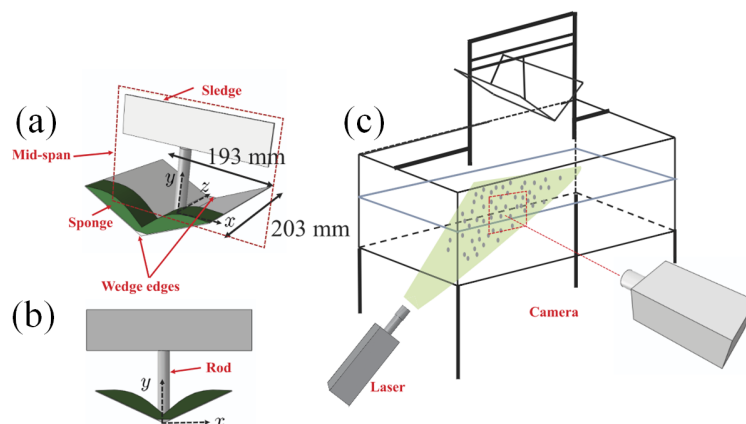


Figure 7. Lifting platform used by Adel Shams to test the water entry–exit of a wedge-shaped body. Reproduced from [65] with permission from AIP Publishing/2024. (a) Schematics of the PIV system, illustrating the positioning of the camera and laser; (b) schematics of the wedge; and (c) front view of the wedge.

In 2020, Tassin et al. [88] conducted experiments with symmetrical bodies (discs, cones, and spheres) in order to study the evolution of the wetted area and the forces on the object during water exit ($U_{\max} = 0.6$ m/s) and water entry–exit. Tassin redesigned the experimental setup first proposed in [89] using a fully transparent experimental model and LED edge illumination device (Figure 8), allowing the size of the wetted area and the forces on the object to be clearly captured. The following conclusions were drawn from the experimental results:

- (1) The shape of the object has no significant effect on the evolution of the wetted area during water exit.
- (2) Experiments with different initial submerging depths and different Fr number show that the surface tension and viscosity have no significant effect during water exit.
- (3) The evolution of the wetted region in the water exit stage of the water entry–exit process is very similar to that of the pure water exit process.
- (4) The theoretical solution obtained from the improved von Karman model does not agree well with the experimental results for water exit. When gravity is neglected, the theoretical solution obtained from the linearized water exit model (at $\lambda = 1$) agrees well with the experiment in the early stages of water exit; nonetheless, the theoretical values in the submerged region are slightly higher than the experimental values due to the effect of gravity.

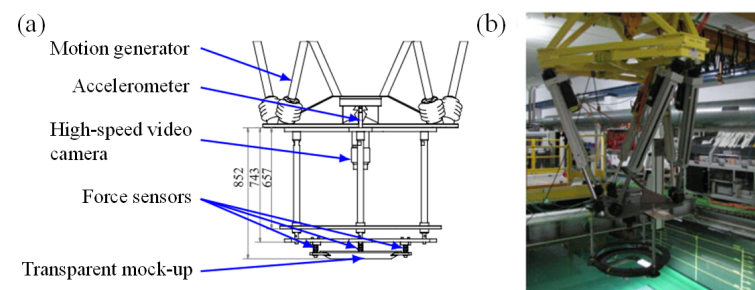


Figure 8. Equipment of the experiment with symmetrical bodies by Tassin. Reproduced from [89] with permission from Cambridge University Press/2024. (a) Schematics of the system and (b) picture of the experimental setup.

In water exits at low speed, it is not easy for objects to produce cavitation; moreover, carrying out high-speed water exit experiments is also not an easy task. To overcome this dilemma, Ren et al. [90] conducted a large number of hemispherical-headed elongated body ($L = 301.4$ mm, $D = 55$ mm) water exit experiments with uniform velocity (0–3.36 m/s) based on a novel depressurized underwater navigational experimental setup by adjusting the ambient atmospheric pressure to 5000 Pa–10,000 Pa. The effects of the Fr number and the cavitation number σ on the generation, development, and collapse of natural bubbles during the water exit of slender bodies were analyzed and the four stages of vacuole water exit collapse were observed and summarized: top contact of bubbles, propulsive collapse, simultaneous collapse, and jet rebound. The experimental results showed that the Fr number mainly has an effect on the shape of the bubble, which is called “bubble cavitation” when the Fr is low and “sheet cavitation” when it is high. On the other hand, the cavitation number σ mainly affects the size of the bubbles.

3.2. Active Water Exit

Compared with forced water exit experiments, the main difficulty in conducting active water exit experiments lies in how to give the object sufficient initial velocity for water exit without disturbing the fluid field. In recent years, scholars have done a great deal of pioneering work on this topic.

Shi et al. [73] conducted experiments on 20 mm, 25 mm, 30 mm, and 50 mm length nails with vertical water exit at initial speed of 14–30 m/s through their self-designed

super-cavity generation device. The evolution of the velocity was obtained (Figure 9), the jump in velocity after water exit was captured, and the cavity generation, evolution, and collapse process was analyzed.

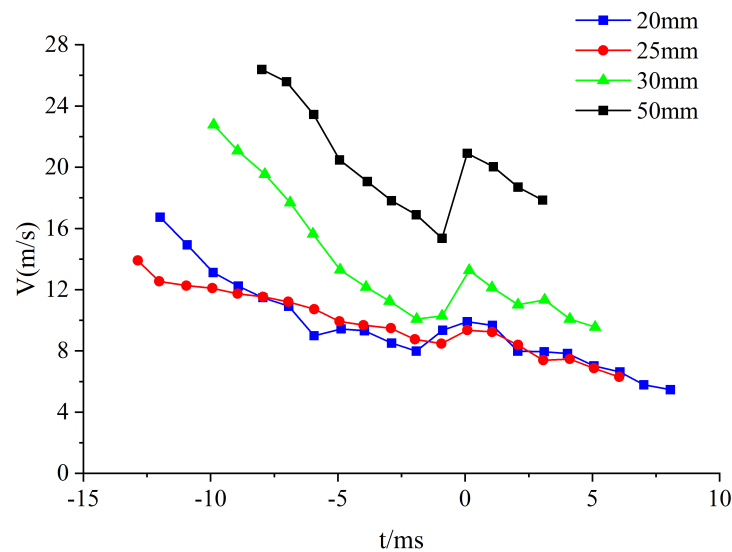


Figure 9. Velocity evolution diagram of nails with different lengths by Shi [73].

Furthermore, Shi et al. [79] conducted water exit experiments on slender blunt-headed nail bodies with length–diameter ratios of 8–12 at different initial velocities (23–29 m/s) and different attack angles using a self-designed water exit device with super-cavity generation capability. Their experiments obtained the velocity and drag coefficient evolution and captured the velocity jumping phenomenon after water exit, which can be explained theoretically through the equations of motion and momentum conservation. Subsequently, their group conducted vertical water exit experiments with high-speed (41.03–79.32 m/s) projectiles [74] with different head types (Figure 10) on the basis of the developed high-speed projectile water exit experimental setup, obtaining the velocity variation curves. Accordingly, the empirical formulas for the cavitation number σ and drag coefficient C were fitted based on the empirical formulas obtained by Reichardt [91] and Logvinovich [92]. Shi et al. [93] continued to further study the cavity evolution of the water exit process of high-speed projectiles with a richer projectile head type (Figure 10). Furthermore, by increasing the projectile velocity (100–150 m/s) based on the experimental setup of high-speed projectiles, the velocity, drag, and cavity displacement variation curves of the projectile were obtained. The experimental results showed that the velocity of projectiles with hemispherical-type heads decays the least and that their cavity diameter is also the least, while the blunt disk type decays the most and has the greatest cavity diameter. The projectile velocity is almost constant after water exit for all types, which is consistent with the theoretical results obtained by May [94].

The study of the water exit problem of a rotating body with initial horizontal velocity is of great importance in military applications; still, few relevant experiments have been conducted. The experimental study of a rotating body by Lu et al. [95] has filled the gap in this area. Based on their own experimental facilities, Lu experimentally studied cavity evolution and ballistic characteristics during the vertical water exit of single-launch and twin-launch rotating bodies at an initial velocity of 15 m/s. In addition, they studied the effect of the initial horizontal velocity (0.5 m/s) by controlling the movement of the underwater launch base (Figure 11). Their results (Figure 12) showed that the cavity and ballistic characteristics of the first shot are essentially the same as those of the single shot, while the development of the cavity of the second shot is significantly asymmetric due to the effects of the first shot. With an initial horizontal velocity, the trajectory revolution of

the second shot is less deflected by the combined effect of pressure difference and initial velocity compared with the first shot under the same condition.

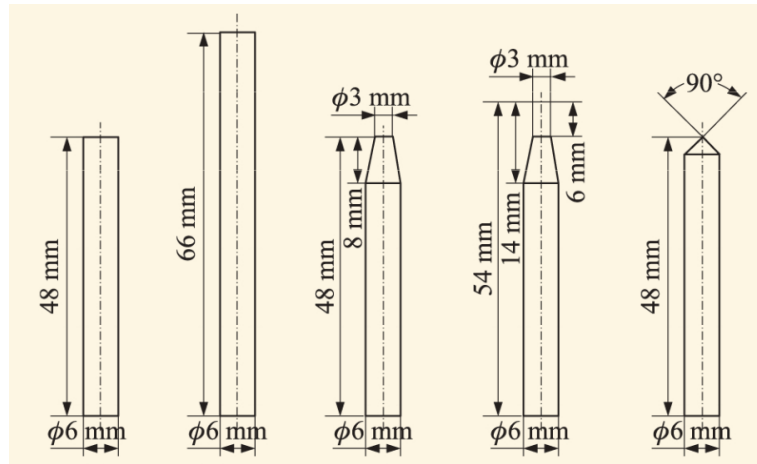


Figure 10. Model parameters of each head shape (2017) [74].

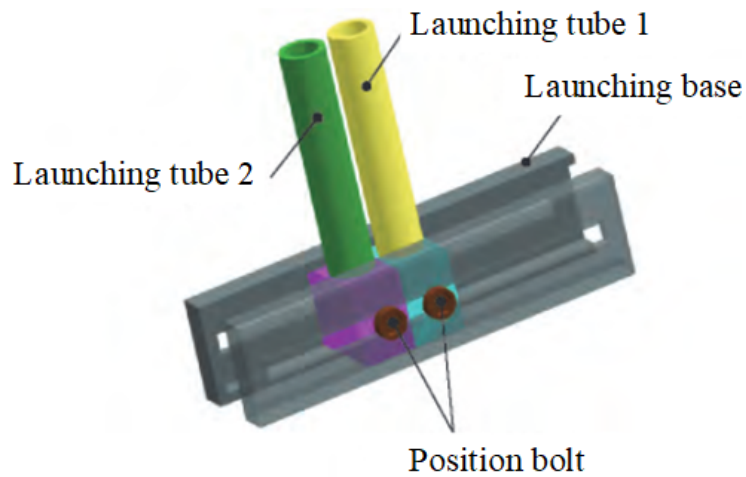


Figure 11. Connection mode of launcher and launching base in Lu's experiment [95].

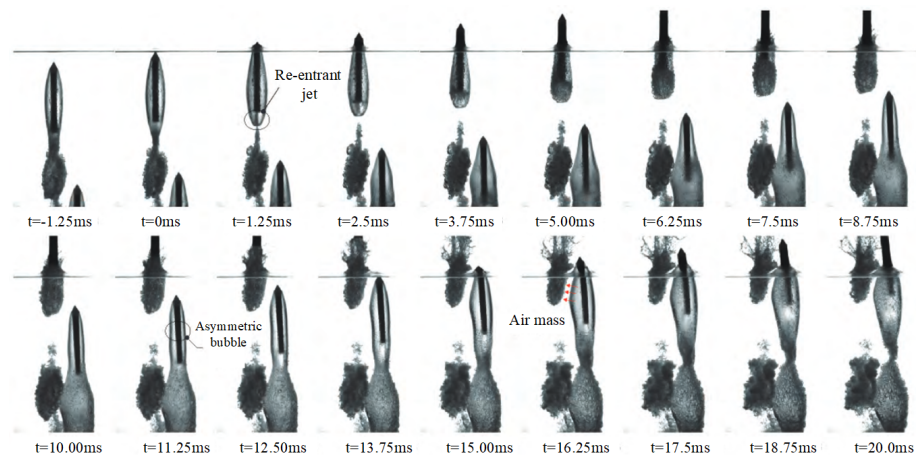


Figure 12. Water exit process of salvo of revolving bodies in Lu's experiment [95].

3.3. Cavitation

From some of the aforementioned experiments, it can be observed that cavitation accompanies the process of water exit, exerting a significant impact on the trajectory and load.

In engineering practice, cavitation has a wide range of applications in fields such as noise reduction, drag reduction, and preventing the destruction of structures [96–99], making it the focus of engineers and scientists. Recent numerical and experimental studies indicate that the formation and collapse of cavities as well as the influence of the free surface on the exit trajectory of objects are of significant importance in various engineering applications. Nguyen et al. [100] investigated the unsteady cavitation phenomenon as objects traverse the free surface, highlighting that the asymmetric pressure effects caused by cavitation collapse represent critical factors affecting the stability of the objects [99,101]. Additionally, horizontal and oblique launches have different effects on the formation, shedding, and collapse of cavitation. For example, the study in [99] explored the impact of different oblique launch angles on cavitation development. It was found that cavitation instability is more pronounced at smaller oblique angles, leading to more intense collapses, which may cause greater disturbances to the object's trajectory and motion stability [99]. In contrast, during vertical launches the motion of the object is more symmetrical and the formation and shedding of cavitation are relatively more orderly. For instance, in vertical launches the cavitation at the rear of the object is less affected by the air–water interface, whereas in oblique launches cavitation shedding and collapse are more significantly influenced, making attitude control more complex [99,101].

However, the occurrence of cavitation and the development of trajectory and morphological transformations of cavitation are rendered highly complex by factors including size, velocity of objects as well as the flow field, making research into cavitation challenging. The processes of water entry and exit both involve complex fluid dynamics as objects traverse the free surface, but differ significantly in cavitation formation and shedding, surface pressure distribution, and flow disturbance. During water entry, cavitation bubbles form due to the cavitation effect as the object contacts the water surface, continuing to develop as the object descends and eventually collapsing. In contrast, during water exit bubbles typically form at the rear of the object as it moves upward, then collapse violently as it crosses the water surface [51,101]. Additionally, cavitation formation and development during water exit are strongly influenced by the air–water interface, generating significant surface tension effects as the object crosses the interface. This differs from water entry, where cavitation forms gradually after the object enters the water under the influence of hydrostatic pressure and object speed, making it comparatively more stable [99].

3.3.1. Formation of the Cavitation

The causes of cavitation around spacecraft include many factors, and the current academic community has not yet reached a clear and complete conclusion on the mechanism of occurrence. Factors such as temperature, liquid compressibility, flow velocity, viscosity, cavitation nuclei, solid wall properties, and local static pressure all have significant impacts on cavitation. Among these, cavitation nuclei and local static pressure play key roles in cavity formation [102].

Unlike phase change processes such as evaporation and boiling, cavitation occurs inside a liquid or near the boundary of an object. Cavitation can only occur when the pressure of the liquid drops below the saturated vapor pressure at the current temperature [103]. Experimental results have shown that in certain cases, such as stationary pure liquids, cavitation is difficult to trigger even if the pressure drops below the saturated vapor pressure at the current temperature. Thus, another necessary condition for cavitation is the existence of cavitation nuclei. The existence of cavitation nuclei reduces the tensile strength of the liquid at the current temperature, creating a weak point inside the liquid, for which Knapp [103] and Harvey [104–106] conducted a series of experiments and provided explanations. When the liquid pressure drops below the saturated vapor pressure, cavitation occurs at the weak point, i.e., the cavitation nuclei; the main components of cavitation nuclei in the liquid are free bubbles of non-condensable gases, which provide the basic conditions for cavitation and have become a consensus topic in the field of cavitation research [107].

3.3.2. Description of Cavitation

In order to better describe the cavitation state and characterize the dynamic similarity index of cavitation, the cavitation number was proposed by [108]:

$$\sigma_{TH} = \frac{P_0 - P_v}{\rho V_0^2 / 2} \quad (5)$$

where P_0 and V_0 respectively represent the reference pressure and reference flow velocity of the liquid at a point where it is not disturbed by the moving object, P_v is the saturated vapor pressure at the current temperature, and ρ is the liquid's density.

The cavitation number can represent the similarity of cavitation scenes between two water flow systems under certain conditions. With the Reynolds number, Weber number, and other similarity criteria being equal, if the cavitation numbers of the two water flow systems are also the same then it can be theoretically considered that their cavitation phenomena are the same. In practice, however, cavitation phenomenon at the same cavitation number may show significant inconsistencies when the size ratio of the two water flow systems changes, exhibiting a clear "scale effect" [109]. In the sub-cavitation flow field, if the cavitation number is reduced by only lowering the pressure or increasing the flow velocity until the flow field shows tiny visible cavities, this state can be identified as "incipient cavitation", and the corresponding cavitation number at this moment is called the "incipient cavitation number". However, during the experimental process it was found that these values are quite dispersed and have poor repeatability due to factors such as water quality and flow conditions. Hence, the cavitation number σ_i is considered more suitable as a sign of cavitation occurrence due to its good repeatability [110,111].

3.3.3. Types of Cavitation

Considering physical characteristics and conditions of occurrence, cavitation can be classified into four types: traveling cavitation, fixed cavitation, vortex cavitation, and vibratory cavitation [103]. According to the cavitating state inside the water and near the solid boundary, cavitation can also be classified into the states of sub-cavitation (cavitation has yet to occur), critical cavitation (cavitation is beginning to occur), local cavitation (cavitation is occurring inside the water or near the solid boundary), and super-cavitation [112]. Self and Ripken et al. [113] conducted experiments on the relationship between the cavitation number and the size of super-cavitation on the surface of a smoothed sphere, with the results indicating that the relationship is less influenced by the scale effect.

3.4. Discussion

Thanks to the efforts of scholars, experimental devices for studying water exits involving various types of objects (flat, blunt, conical) and different velocities have been designed. The typical phenomena during a water exit, such as liquid surface lift, liquid surface-breaking, cavity generation and evolution, and velocity jumps, can now be clearly captured. In addition to PIV, depressurized setups, super-cavity generation devices, and other experimental technical means are emerging, with the potential to greatly promote research on the water exit problem and provide reliable and real data for both theoretical research and numerical simulations. Existing experimental equipment has enabled effective observation and analysis of many phenomena and data concerning the water exit process, and some of the results can provide guidance for industrial and military applications. However, due to the cost and the difficulty of experiments, the size and exiting speed of the object are always scaled, which is different from practice. Furthermore, there is a lack of effective experimental studies on the structural force response of objects under fluid–structure coupling, which is an important concern in engineering applications. Above all, improvements and breakthroughs can be made in a number of aspects when redesigning experimental equipment and carrying out water exit experiments:

(1) In actual situations, the hydrological conditions that navigators face are extremely complex, accompanied by wave surges, ocean currents and even strong winds rather than being as calm as in an experimental tank. To address this, wave-makers can be used to simulate different hydrological conditions when conducting water exit experiments in order to study the water exit process. If this can be done, it will help to establish a test station in a real water area [40].

(2) Many countries have paid attention to drag reduction through super-cavitation. However, the speed of the object in water exit experiments is usually not high enough to produce super-cavitation that can cover the whole body. In current experiments, cavitation is mainly induced passively by one of two means: adjusting the ambient atmospheric pressure in the depressurized setup, or increasing exit speeds while significantly reducing the size of the object. Active cavitating technology at different speeds and sizes has wide application in engineering, and ensuring the stability and controllability of the object in a super-cavitating state is a current research focus. The development of relevant experimental equipment is of great significance in solving this problem.

(3) At present, most water exit experiments regard the object as a whole body, and the overall force and motion parameters receive the most attention. However, impacts or even damage to the local structure of the object have not been widely considered. Therefore, ways to monitor the stress response of the object structure is another area worthy of further research.

4. Numerical Simulation

Due to its low cost, high efficiency, and good flexibility, numerical simulation provides unique advantages that make it an indispensable tool for solving engineering problems today. Therefore, many scholars have carried out numerical research on the water exit problem [26,114–116]. In 1965, Moran [117] reviewed the mathematical theory of the water exit process and concluded that it was difficult to accurately calculate the loads on the object during water exit in theory, instead suggesting that the NS equation be solved by numerical simulation and then compared with experimental results. However, the physical processes involved in the water exit process are rather complicated when the liquid surface breaks up and the water body separates, with which mesh distortion occurring when traditional numerical methods are performed. The latest numerical methods, such as BEM, usually terminate when the liquid surface breaks up [75], while meshless methods such as SPH [118] are unable to effectively simulate the whole process of water exit due to numerical oscillations.

Several numerical methods that have been used successfully in the numerical simulation on the water exit problem are introduced in this section, namely, BEM, VOF (Volume of Fluid), and FVM (Finite Volume Method).

4.1. BEM Method

The theoretical basis of the BEM method is integral equation theory, inspired by the idea of discretization from FEM (Finite Element Method). Unlike FEM, BEM is a boundary-type numerical method that discretizes the integral boundary equation into a group of algebraic equations by dividing the mesh on the boundary of the calculation region, which is also the most important feature of BEM, namely, dimension reduction. Through the BEM method, spatial and planar problems can be respectively transformed into two-dimensional problems on the boundary interface of the calculation region and one-dimensional problems on the boundary line. Compared with region-based numerical methods such as FEM and FDM (Finite Difference Method), in the BEM it is only necessary to divide the mesh on the boundary rather than discretize in the whole region. Thus, not only can the dimension of the problem be reduced, the difficulty of discretizing models is overcome as well. Therefore, BEM has a great advantage in solving problems with complex boundaries, interfaces, and shapes, and has been considered for application in the solution of water exit process problems by many scholars.

Early in 1976, Longuet et al. [119] used the axisymmetric BEM to carry out a preliminary exploration of the process of neutral objects penetrating the free liquid surface. Ye [120] applied nonlinear boundary conditions in order to numerically calculate the vertical water exit problem of an axisymmetric object of arbitrary shape using the BEM. Later, based on the small-angle regression method, Ye et al. [47] also studied the three-dimensional water exit problem and the process of water exit until approaching the free liquid surface by conducting simulations using the BEM. Greenhow and Moyo [45] and other scholars [121] studied the two-dimensional forced vertically water exit problem of a cylinder with uniform velocity under both full and semi-submerged conditions using the BEM. Their studies analyzed the free liquid surface deformation phenomenon and compared it with the analytical solution based on the small-time expansion method by Peder et al. [122], which were in good agreement. Liju et al. [75,123] used the BEM to investigate the water exit problems of a two-dimensional axisymmetric object with constant velocity and constant acceleration conditions. Until then the numerical simulations of the water exit problem by the BEM method had been numerically terminated prior to the breakup of the free surface or the penetration of the object into the liquid surface. The reason for this is that the water layer at the front of the object becomes thinner and thinner as the object rises before the object penetrates the liquid surface and the liquid surface breaks up. During this process the scale of the physical problem decreases to the micron level [75], making both experimental image capture and numerical calculations challenging.

Inspired by [124,125], Wu et al. [49] proposed the liquid surface fragmentation and solid-liquid separation algorithm, which was applied to the BEM by setting the minimum water layer thickness (as shown in Figures 13 and 14) as the criterion between liquid surface fragmentation and water body separation. The whole process of water exit of a light ellipsoid with different ratios was successfully simulated, including the phenomena of free liquid surface breaking, water body separation, free surface oscillation, and jet development, all of which were successfully captured while obtaining good convergence [48].

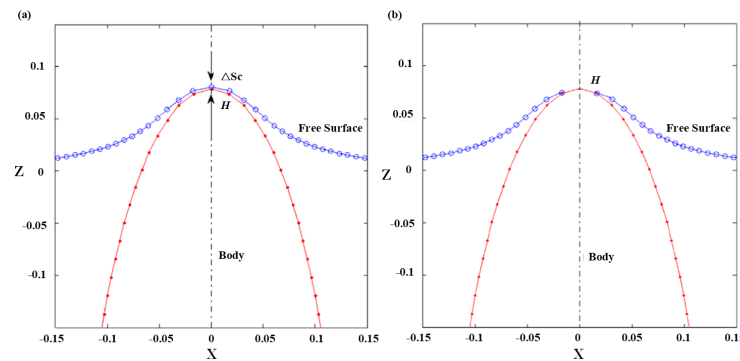


Figure 13. Sketch of the numerical procedure for breakup of the water layer by Wu. Reproduced from [49] with permission from Elsevier/2024. (a) Before breakup and (b) after breakup.

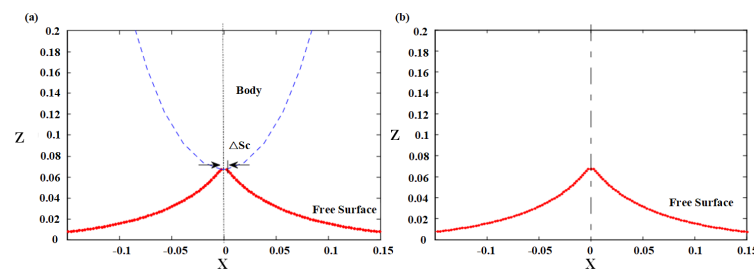


Figure 14. Sketch of the numerical procedure for liquid detachment from the body surface by Wu. Reproduced from [49] with permission from Elsevier/2024. (a) Before detachment and (b) after detachment.

However, in order to use the BEM method to calculate the water exit problem, the velocity of the object needs to be low (less than 10 m/s). Therefore, the phase change and cavitation phenomena arising from high-velocity water exit processes have not been nearly as well studied.

4.2. VOF Method

As a well-established numerical method, the VOF method is widely used in fluid–solid coupling, multiphase flow, and heat transfer problems. Therefore, many scholars have also applied it to the water exit problem.

Tassin et al. [63] used the VOF solver in OpenFoam to solve the gas–liquid two-phase flow. The dynamic grid technique was applied to solve the fluid–solid interaction problem of a moving object. The water entry and water exit problems for wedges with shapes that can change with time were simulated and agreed well with the forces predicted by the theoretical solution; however the theoretical solution of the water exit stage did not always match the numerical solution. Based on the OpenFoam open-source library, Piro et al. [67] used the FEM method for the fluid–solid weak coupling problem and the VOF method for the free interface problem, in which the fluid was assumed to be laminar and incompressible. Numerical calculations were performed for rigid and elastic wedges with constant acceleration in water entry and water exit problems, respectively, regardless of the effects of gravity, viscosity, and turbulence. Comparing the numerical solution of the force and splash location of the object during water entry with the theoretical solution of Wanger [7,36] and the numerical solution of the wetted region during water exit with the theoretical solution [6], good agreements were achieved.

Shi [79] applied the VOF multiphase flow model, the Schnerr–Sauer cavitation model, and the mesh reconstruction method to numerically simulate the slender body water exit problem, in which the generation and evolution of cavitation and the water pressure changes were analyzed. However, the cavitation model was a natural cavitation model and the effect of the interaction with the atmosphere on cavitation after the object water exit was not considered. Meanwhile, based on the data obtained by specific speed (41.03 m/s–79.32 m/s) projectile experiments as known conditions, [74] applied the dynamic mesh technique and the VOF multiphase flow model to calculate slender body high-speed water exit problems in which the turbulence was considered. The cavity-shedding and water splashing behaviors were in good agreement with experiment.

Based on ANSYS CFX 14.0 with the SST k - ω turbulence model and VOF method to capture the free liquid surface, Ma et al. [126] established a model for the cross-media motion of a slender body and numerically calculated the slender body water exit problem. The effects of the attack angle and angular velocity on the attitude of water exit were investigated. Compared with the results of the BEM and experimental results, the velocity, acceleration, and attack angle variation patterns were all in good agreement and the velocity jump at the end of the water exit was observed. With the VOF method, Shi [93] used the Schnerr–Sauer cavitation model and 6-DOF method to investigate the super cavitation problem during water exit with different head types, with the results being generally consistent with experimental phenomena. The velocity and displacement evolution of the cavitation projectile during the water exit process were compared with the experimental data and semi-empirical formulae, finding good agreement.

4.3. FVM Method with LES

Turbulence has a significant effect on energy exchange, dissipation, and Reynolds stress. During the process of water exit, when the object's velocity increases, the Reynolds number increase as well; thus, the turbulence becomes more obvious. Normally, VOF, BEM, and other methods are not sufficiently advantageous in turbulent flow simulation. In order to simulate turbulent flow, it is necessary for the size of the computational region to be large enough to contain the largest vortices in the turbulent flow, while the size of the computational mesh should be small enough to distinguish the motion of the smallest

vortices. Large-scale eddies have a large effect on the mean flow, while small-scale eddies mainly play a role in dissipation. At present, the minimum scale of the computational mesh is still much larger than the scale of the smallest eddy, making it difficult to perform direct full-scale simulations. This resulted in the LES (Large Eddy Simulation) model. The LES is based on an isotropic grid, uniform octree filtering, and a high-resolution interface capture algorithm [26]. The whole process of a submarine-launched missile from water into air was simulated by Chen using FVM with the LES model [127] (see Figures 15 and 16). The effects of launch depth, angle of attack, and initial velocity on the flow field around the projectile and the evolutionary development pattern of the cavity were explored.

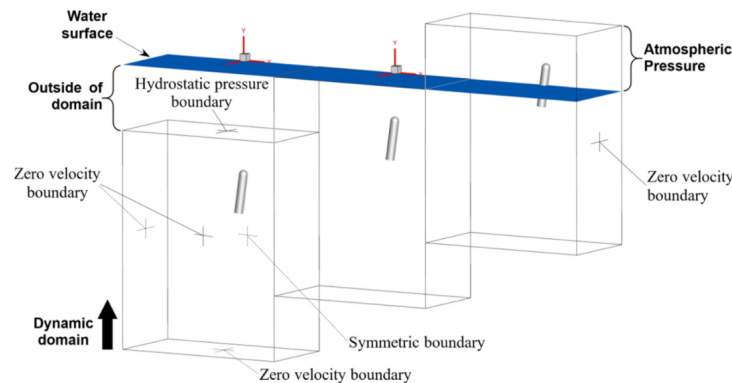


Figure 15. Schematic diagram of the dynamic computational domain and the boundary condition by Chen. Reproduced from [127] with permission from Elsevier/2024.

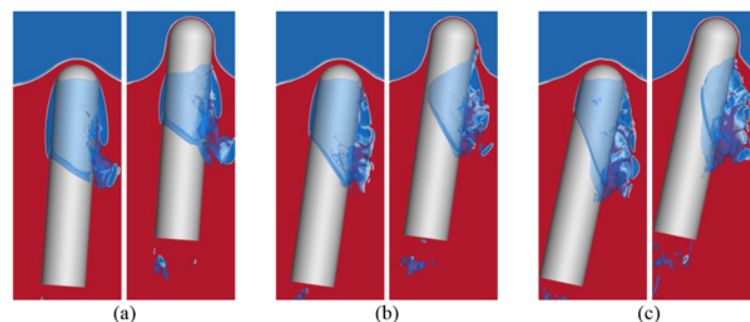


Figure 16. Asymmetric cavitation interface at different water exit angles of attack by Chen. Reproduced from [127] with permission from Elsevier/2024. (a) $H = 10 L$, $AOA = 4^\circ$, $V = 35 L/s$; (b) $H = 10 L$, $AOA = 8^\circ$, $V = 35 L/s$; (c) $H = 10 L$, $AOA = 12^\circ$, $V = 35 L/s$.

4.4. Discussion

In addition to the above-mentioned studies, other scholars have achieved results with the FDM and SPH methods. In order to simulate cavity generation and evolution during the water exit process, the BUBMAC method [128] and FLUENT multiphase flow cavitation model [129] have been used to numerically calculate the water exit problem of a long cylinder. Regarding the cylindrical and free-surface action problem as a multiphase flow, Zhu et al. [121] used the FDM method based on CIP (Constrained Interpolation Profile) to numerically simulate the two-dimensional horizontal cylindrical water exit and water entry problem. Among these, the numerical results of a water exit subjected to constant force were compared with the experimental results in [44], finding that the phenomena and displacement evolution both agreed well. The numerical results of a uniform water exit were compared with the experimental results in [46], finding that the impact coefficients were well matched. Jafar et al. [130] applied the SPH method to simulate the water exit problem of a two-dimensional rotating cylinder with the SPS turbulence model. The effects of the parameters such as depth, column density, vertical velocity, and horizontal velocity on the vortices, velocity components of the flow field, and free

liquid surface of the cylindrical wake were analyzed. Wu et al. [131] studied the water exit problem of a slender body with SPH method to investigate the effect of different motion parameters on the hydrodynamic characteristics by changing the velocity and the attack angle. In addition, Josip [132] and other scholars used the ISPH (Incompressible SPH) method to numerically simulate the water exit problem of a cylinder with constant velocity, then analyzed the resulting free liquid surface motion and force evolution law.

The influence of hydrodynamic loads on the stress response and distribution of the structural body during water exit is of great importance for the design of structural bodies. To address the problem of treating the water exit object as elastic rather than rigid, Hu et al. [133] combined a flow field solver based on the FVM and a structural solver based on the FEM to study the water exit problem of an elastic flat-headed cylindrical shell with cavitation at a certain attack angle. The deformation characteristics of the structure under the action of hydrodynamic loads and the coupling relationship between the hydrodynamic properties and structural vibrations were demonstrated in their research.

Although many numerical studies have been conducted on the water exit problem, several problems still exist related to the following aspects. First, study of the water exit problem for elastic bodies is relatively limited; to the best of our knowledge, only Hu's research [133] has addressed this topic. Second, the velocities dealt with in water exit problems have typically been low (below 50 m/s), with higher velocities (above 50 m/s) rarely being studied.

5. Conclusions

The water exit problem is one of the most critical topics in the study of interactions between navigable bodies and water flows, and is of great significance for marine ships and underwater vehicles. Numerous scholars have extensively investigated this issue from various perspectives, yielding substantial findings. In this paper, we have provided a comprehensive review of these findings from three aspects: theoretical research, experimental development, and numerical simulations. The research outcomes are systematically organized and analyzed according to a problem-oriented framework.

In summary, theoretical research, experimental studies, and numerical simulations all offer distinct advantages and face specific limitations when addressing the water exit problem. Theoretical research provides a foundational understanding of the mechanisms involved, with models such as the improved von Karman and linearized models offering simplified predictions at low computational cost. However, their accuracy is constrained by simplifications and assumptions, limiting their applicability to complex phenomena such as cavitation and multiphase flows. Experimental studies offer direct observation of key phenomena and provide critical empirical data to validate theoretical and numerical models. The use of advanced technologies such as PIV and LED edge lighting has improved data acquisition. Nonetheless, experiments are costly and complex to execute, especially at high velocities or under real-world conditions, and capturing fluid–structure interactions remains a significant challenge. Numerical simulations, on the other hand, provide high efficiency and flexibility, allowing for detailed modeling of multiphase flows, cavitation, and fluid dynamics through methods such as BEM, VOF, and FVM. Despite their advantages, numerical simulations are constrained by mesh distortion, computational instability, and limited ability to fully capture phenomena such as phase changes and fluid–solid interactions. Therefore, future research should aim to integrate the strengths of all three methods to overcome their individual limitations and provide a more comprehensive and accurate understanding of the water exit problem.

In the future, research on the water exit problem should focus on several critical areas. First, advancements in theoretical models are needed to extend current 2D models to 3D scenarios while incorporating nonlinear effects, gravity, viscosity, and phenomena such as cavitation and surface fragmentation. Second, experimental methods should evolve with more sophisticated techniques to better capture high-speed water exit processes and complex hydrological conditions such as wave action and ocean currents. Developing

cost-effective and realistic experimental setups, possibly in open-water or wave tank environments, will be crucial for providing reliable data for model validation. Third, numerical simulations can be significantly improved by integrating mesh-based and meshless methods, such as combining FVM with SPH. This would allow for more accurate simulation of multiphase flows and fluid–structure interactions, particularly at higher velocities. Finally, further research into cavitation dynamics, bubble growth, and their impact on structural integrity during water exit is essential for improving the stability and performance of marine structures and underwater vehicles. By advancing these areas in a coordinated manner, future research can provide more comprehensive and practical solutions for marine engineering and underwater technology applications.

Author Contributions: Investigation, H.Z.; data curation, H.Z.; writing—original draft preparation, H.Z.; writing—review and editing, H.Z. and Y.Z.; visualization, H.Z.; supervision, H.Q. and C.Z.; project administration, Y.Z.; funding acquisition, Y.Z. and H.Q. All authors have read and agreed to the published version of the manuscript.

Funding: This research was funded by the national natural science foundation of China (Grant Nos. 12302383, 92152201, 52375559), the National Natural Science Foundation of Shaanxi Province (Grant No. 2023-JC-QN-0052), the Postdoctoral Science Foundation (Grant No. 2023M734284), and the Youth Talent Support of Shaanxi Province (Grant No. 20230519).

Institutional Review Board Statement: Not applicable.

Informed Consent Statement: Not applicable.

Data Availability Statement: Not applicable.

Acknowledgments: The authors acknowledge technical support from Zhijian Laboratory of Xi'an Research Institute of High Technology. We are grateful to the anonymous referees and to the editor, who provided valuable comments that improved the manuscript.

Conflicts of Interest: The authors declare no conflicts of interest.

Disclaimer: Current research is limited to the water exit problems in civilian contexts of ocean engineering, which benefits maritime safety as well as environmental sustainability and does not pose a threat to public health or national security. The authors acknowledge the dual-use potential of research involving direct military applications, and confirm that all necessary precautions have been taken to prevent potential misuse. As an ethical responsibility, the authors strictly adhere to all relevant national and international laws concerning DURC. The authors advocate for responsible deployment, ethical considerations, regulatory compliance, and transparent reporting to mitigate misuse risks and foster beneficial outcomes.

References

1. Kuklinski, R.; Castano, J.; Henoach, C. Experimental Study of Ventilated Cavities on Dynamic Test Model. In Proceedings of the Fourth International Symposium on Cavitation (CAV 2001), Pasadena, CA USA, 20–23 June 2001.
2. Cong, M.; Wei, G. Supercavitation Research Program of the US Navy. *Aerodyn. Missile J.* **2009**, *1*, 17–20.
3. Zhu, J. Current Status of Research on German Supercavitation Underwater Weapons. *Mine Warf. Ship Prot.* **2005**, *4*, 12–17.
4. Kulkarni, S.S.; Pratap, R. Studies on the dynamics of a supercavitating projectile. *Appl. Math. Model.* **2000**, *24*, 113–129. [[CrossRef](#)]
5. Yao, G.; Li, Y.; Zhang, H.; Jiang, Y.; Wang, T.; Sun, F.; Yang, X. Review of hybrid aquatic-aerial vehicle (HAAV): Classifications, current status, applications, challenges and technology perspectives. *Prog. Aerosp. Sci.* **2023**, *139*, 100902. [[CrossRef](#)]
6. Karman, T.V. *The Impact of Seaplane Floats during Landing*; Technical Report; Archive and Image Library: Chicago, IL, USA, 1929.
7. Wagner, H. Phenomena Associated with Impacts and Sliding on Liquid Surfaces. *ZAMM J. Appl. Math. Mech.* **1932**, *12*, 193–215. [[CrossRef](#)]
8. Kaplan, P. Analysis and prediction of flat bottom slamming impact of advanced marine vehicles in waves. *Int. Shipbuild. Prog.* **1987**, *34*, 44–53. [[CrossRef](#)]
9. Wei, Y.; Min, J.; Wang, C.; Zou, Z.; Yu, F. Research on cavitation of vertical launch submarine missile. *Eng. Mech.* **2009**, *26*, 251–256.
10. Min, J.; Wei, Y.; Wang, C.; Cao, W.; Zou, Z. Numerical Simulation on Hydrodynamic Characteristics of Submarine Missile in the Vertical Launch Process. *Acta Armamentarii* **2010**, *31*, 1303–1309.
11. Liu, H.; Wang, C.; Zou, Z.; Wang, B.; Wang, B. Numerical investigation on the hydrodynamic characteristics of a cylinder of different head construction out of launch tube. *J. Harbin Eng. Univ.* **2012**, *33*, 6.

12. Li, R. Research on the Flow Field and Ballistic Characteristics of the Gas-Steam Ejection. Ph.D. Thesis, Nanjing University of Science and Technology, Nanjing, China, 2019.
13. Zhao, Y. The Research on Hydrodynamic Characteristics of Sharing Launched Submaring-Launched Vehicle. Ph.D. Thesis, Harbin Institute of Technology, Harbin, China, 2014.
14. Shang, R. Numerical Simulation on Hydrodynamics Characteristics of Ventilating Submaring-Launched Vehicle in the Vertical Launch Process. Ph.D. Thesis, Harbin Institute of Technology, Harbin, China, 2013.
15. Liu, Z.; Yan, K.; Wang, B. Numerical simulation of the development process of a trailing cavity from generation to separation. *J. Ship Mech.* **2005**, *9*, 8.
16. Chen, W.; Wang, B.; Yan, K.; Yi, S. Research on Unsteady Vertical Cavitation in Cavitator Effluent. *Chin. J. Theor. Appl. Mech.* **2013**, *45*, 7.
17. Kozelkov, A.S.; Kurkin, A.A.; Pelinovskii, E.N. Effect of the angle of water entry of a body on the generated wave heights. *Fluid Dyn.* **2016**, *51*, 288–298. [[CrossRef](#)]
18. Zhao, K.; Yang, S.F.; Ming, F.R. Numerical analysis of water entry under ocean currents with smoothed particle hydrodynamics method. *Phys. Fluids* **2023**, *35*, 062103.
19. Wu, X.; Chang, X.; Liu, S.; Yu, P.; Zhou, L.; Tian, W. Numerical Study on the Water Entry Impact Forces of an Air-Launched Underwater Glider under Wave Conditions. *Shock Vib.* **2022**, *2022*, 4330043. [[CrossRef](#)]
20. Sun, J.Y.; Sun, S.L.; Zhang, Z.L.; Ren, H.L. Water entry of a seaplane section considering the wave effect. *Phys. Fluids* **2024**, *36*, 082115. [[CrossRef](#)]
21. Chen, C.W.; Wang, T.; Feng, Z.; Lu, Y.; Huang, H.; Ji, D.; Chen, Y. Simulation research on water-entry impact force of an autonomous underwater helicopter. *J. Mar. Sci. Technol.* **2020**, *25*, 1166–1181. [[CrossRef](#)]
22. Chaudhry, A.Z.; Pan, G.; Shi, Y. Numerical evaluation of the hydrodynamic impact characteristics of the air launched AUV upon water entry. *Mod. Phys. Lett. B* **2020**, *34*, 2050149. [[CrossRef](#)]
23. Shi, Y.; Gao, X.; Pan, G. Experimental and numerical investigation of the frequency-domain characteristics of impact load for AUV during water entry. *Ocean Eng.* **2020**, *202*, 107203. [[CrossRef](#)]
24. Rosellini, L.; Hersen, F.; Clanet, C.; Bocquet, L. Skipping stones. *J. Fluid Mech.* **2005**, *543*, 137–146. [[CrossRef](#)]
25. Bush, J.W.M.; Hu, D.L. Walking on Water: Bioloocomotion at the Interface. *Phys. Today* **2006**, *38*, 339–369. [[CrossRef](#)]
26. Khosronejad, A.; Mendelson, L.; Techet, A.H.; Angelidis, D.; Sotiropoulos, F. Water exit dynamics of jumping archer fish: Integrating two-phase flow large-eddy simulation with experimental measurements. *Phys. Fluids* **2020**, *32*, 011904. [[CrossRef](#)]
27. Worthington, A.M.; Cole, R.S. *Impact with a Liquid Surface Studied by the Aid of Instantaneous Photography. Paper II*; The Royal Society: London, UK, 1900.
28. May, A.; Woodhull, J.C. The Virtual Mass of a Sphere Entering Water Vertically. *J. Appl. Phys.* **1950**, *21*, 1285–1289. [[CrossRef](#)]
29. May, A. Effect of Surface Condition of a Sphere on Its Water-Entry Cavity. *J. Appl. Phys.* **1951**, *22*, 1219–1222. [[CrossRef](#)]
30. Wei, Z.; Hu, C. Experimental study on water entry of circular cylinders with inclined angles. *J. Mar. Sci. Technol.* **2015**, *20*, 722–738. [[CrossRef](#)]
31. Truscott, T.; Techet, A. Water entry of spinning spheres. *J. Fluid Mech.* **2009**, *625*, 135–165. [[CrossRef](#)]
32. Sun, L.; Wang, D.; Chen, Y.; Wu, G. Numerical and experimental investigation on the oblique water entry of cylinder. *Sci. Prog.* **2020**, *103*, 0036850420940889. [[CrossRef](#)]
33. Yu, P.; Li, H.; Ong, M.C. Numerical study on the water entry of curved wedges. *Ships Offshore Struct.* **2018**, *13*, 885–898. [[CrossRef](#)]
34. Oliver, J.M. *Water Entry and Related Problems*; University of Oxford: Oxford, UK, 2002.
35. Ni, B.; Wu, G. Numerical simulation of water exit of an initially fully submerged buoyant spheroid in an axisymmetric flow. *Fluid Dyn. Res.* **2017**, *49*, 045511. [[CrossRef](#)]
36. Wagner, H. *Landing of Seaplane, National Advisory Committee for Aeronautics*; Technical Memorandum No. 622; NASA: Washington, DC, USA, 1931.
37. Wang, Z.; Feng, J.; Cheng, S.; Wei, H.; You, T. Study on Binary-State Pitching Movement of Water-Exit Trajectory of Underwater Vehicles. *J. Ordnance Equip. Eng.* **2016**, *37*, 163–166.
38. Hu, J.; Xu, B.; Feng, J.; Yang, J.; Wang, C. Research on Water-Exit and Take-off Process for Morphing Unmanned Submersible Aerial Vehicle. *China Ocean Eng.* **2017**, *31*, 202–209. [[CrossRef](#)]
39. Sun, X.; Cao, J.; Li, Y.; Ling, Y. Efficient prediction method for the water-exit characteristics of unmanned aerial–underwater vehicles. *Ocean Eng.* **2024**, *302*, 302. [[CrossRef](#)]
40. Fu, J. Research of German Supercavitation Weapons in the Water. *Mine Warf. Ship Prot. J.* **2005**, *6*, 12–17.
41. Yan, K. Principle and Method of Nuclear Seeding in Cavitating Water Tube—Review of French Research. *J. Ship Mech.* **1999**, *3*, 78–82.
42. Wu, Q.; Wang, L.; Xie, Y.; Du, Z.; Yu, H. Numerical Simulation of the water-exit process of the missile based on Moving Particle Semi-Implicit method. *J. Phys. Conf. Ser.* **2019**, *1300*, 012064. [[CrossRef](#)]
43. Greenhow, M.; Li, Y. Added masses for circular cylinders near or penetrating fluid boundaries—Review, extension and application to water-entry, -exit and slamming. *Ocean Eng.* **1987**, *14*, 325–348. [[CrossRef](#)]
44. Greenhow, M.; Minlin, W. *Nonlinear Free Surface Effects Experiments and Theory*; FAO: Rome, Italy, 1983; pp. 83–119.
45. Greenhow, M.; Moyo, S. Water entry and exit of horizontal circular cylinders. *Philos. Trans. R. Soc. A Math. Phys. Eng. Sci.* **1997**, *355*, 551–563. [[CrossRef](#)]

46. Miao, G. Hydrodynamic Forces and Dynamic Response of Circular Cylinders in Wave Zones. Ph.D. Thesis, Nanjing University of Science and Technology, Nanjing, China, 1988.
47. Ye, Q.; He, Y. Double-parameter perturbation solution to 3-D nonlinear problem of oblique water exit. *J. Hydrodyn.* **1991**, *3*, 96–103.
48. Ni, B.Y.; Zhang, A.M.; Wu, G.X. Simulation of complete water exit of a fully-submerged body. *J. Fluids Struct.* **2015**, *58*, 79–98. [[CrossRef](#)]
49. Wu, Q.G.; Ni, B.Y.; Xue, Y.Z.; Zhang, A.M. Experimental and numerical study of free water exit and re-entry of a fully submerged buoyant spheroid. *Appl. Ocean Res.* **2018**, *76*, 110–124. [[CrossRef](#)]
50. Yang, X.; Feng, S.; Wu, J.; Zhang, G.; Liang, G.; Zhang, Z. Study of the water entry and exit problems by coupling the APR and PST within SPH. *Appl. Ocean Res.* **2023**, *139*, 103712. [[CrossRef](#)]
51. Yun, H.; Liu, Q.; Zeng, Z.; Lian, L. Experimental study on water-exit of cylinder. *Ocean Eng.* **2024**, *293*, 116585. [[CrossRef](#)]
52. Zheng, H.; Qiang, H.; Zhu, Y.; Zhang, C. A parameter-free particle relaxation technique for smoothed particle hydrodynamics. *Phys. Fluids* **2024**, *36*, 097137. [[CrossRef](#)]
53. Zhu, Y.; Zhang, C.; Yu, Y.; Hu, X. A CAD-compatible body-fitted particle generator for arbitrarily complex geometry and its application to wave-structure interaction. *J. Hydrodyn.* **2021**, *33*, 195–206. [[CrossRef](#)]
54. Luo, M.; Khayyer, A.; Lin, P. Particle methods in ocean and coastal engineering. *Appl. Ocean Res.* **2021**, *114*, 102734. [[CrossRef](#)]
55. Wang, H.; Huang, Z.; Cai, X.; Liu, X.; Chen, Z.; Na, X. Analysis of the water-exit cavity evolution and motion characteristics of an underwater vehicle under the effect of floating ice. *Ocean Eng.* **2024**, *300*, 117374. [[CrossRef](#)]
56. Moran, J. Line source distributions and slender-body theory. *J. Fluid Mech.* **2006**, *17*, 285–304. [[CrossRef](#)]
57. Moran, J. Addendum—The vertical water-exit and entry of slender symmetric bodies. *AIAA J.* **1964**, *2*, 1480–1482. [[CrossRef](#)]
58. Moran, J. Image solution for vertical motion of a point source towards a free surface. *J. Fluid Mech.* **2006**, *18*, 315–320. [[CrossRef](#)]
59. Moran, J. The Vertical Water-Exit and -Entry of Slender Symmetric Bodies. *J. Aerosp. Sci.* **1961**, *28*, 803–812. [[CrossRef](#)]
60. Yang, J.; Feng, J.; Li, Y.; Liu, A.; Hu, J.; Ma, Z. Water-Exit Process Modeling and Added-Mass Calculation of the Submarine-Launched Missile. *Pol. Marit. Res.* **2017**, *24*, 152–164. [[CrossRef](#)]
61. Li, J.; Lu, C.; Huang, X. Calculation of added mass of a vehicle running with cavity. *J. Hydrodyn. Ser. B* **2010**, *22*, 312–318. [[CrossRef](#)]
62. Takamura, K.; Uchiyama, T. Calculation model for water mass entrained by the water exit of a particle using two projected images captured from orthogonal directions. *Ocean Eng.* **2022**, *266*, 112848. [[CrossRef](#)]
63. Tassin, A.; Piro, D.; Korobkin, A.; Maki, K.; Cooker, M. Two-dimensional water entry and exit of a body whose shape varies in time. *J. Fluids Struct.* **2013**, *40*, 317–336. [[CrossRef](#)]
64. Piro, D.; Maki, K. Water Exit of a Wedge-Shaped Body. In Proceedings of the 27th IWWFBB, Copenhagen, Denmark, 22–25 April 2012; pp. 141–144.
65. Shams, A.; Zhao, S.; Porfiri, M. Hydroelastic slamming of flexible wedges: Modeling and experiments from water entry to exit. *Phys. Fluids* **2017**, *29*, 037107. [[CrossRef](#)]
66. Korobkin, A.A. A linearized model of water exit. *J. Fluid Mech.* **2013**, *737*, 368–386. [[CrossRef](#)]
67. Piro, D.J.; Maki, K.J. Hydroelastic analysis of bodies that enter and exit water. *J. Fluids Struct.* **2013**, *37*, 134–150. [[CrossRef](#)]
68. Colicchio, G.; Greco, M.; Miozzi, M.; Lugni, C. Experimental and numerical investigation of the water-entry and water-exit of a circular cylinder. In Proceedings of the 24th International Workshop on Water Waves and Floating Bodies, Zelenogorsk, Russia, 19–22 April 2009.
69. Jenny, M.; Duek, J.; Bouchet, G. Instabilities and transition of a sphere falling or ascending freely in a Newtonian fluid. *J. Fluid Mech.* **2017**, *508*, 201–239. [[CrossRef](#)]
70. Moyo, S.; Greenhow, M. Free motion of a cylinder moving below and through a free surface. *Appl. Ocean Res.* **2000**, *22*, 31–44. [[CrossRef](#)]
71. Truscott, T.T.; Epps, B.P.; Munns, R.H. Water exit dynamics of buoyant spheres. *Phys. Rev. Fluids* **2016**, *1*, 074501. [[CrossRef](#)]
72. Bourrier, P.; Guyon, E.; Jorje, J.P. The “pop off” effect: Different regimes of a light ball in water. *Eur. J. Phys.* **1984**, *5*, 225–231. [[CrossRef](#)]
73. Chen, B.; Peng, L.; Shi, H.; Jia, H. Experimental and numerical study on hydrodynamic characteristics in water-exit of slender body. *J. Exp. Fluid Mech.* **2015**, *29*, 26–31. 42.
74. Hou, J.; Shi, H.; Sun, Y.; Gao, J. Study on the Trajectory of High-speed Projectile Exiting From Water. *J. Ballist.* **2017**, *29*, 51–56.
75. Liju, P.Y.; Machane, R.; Cartellier, A. Surge effect during the water exit of an axisymmetric body travelling normal to a plane interface: Experiments and BEM simulation. *Exp. Fluids* **2001**, *31*, 241–248. [[CrossRef](#)]
76. Shi, H.; Chen, S.; Dong, R.; Zhang, L.; Guo, Q.; Jia, H.; Wang, C. Research on the characteristics of momentum jet of underwater supersonic gas. *J. Zhejiang Sci-Tech Univ.* **2012**, *29*, 366–369.
77. Zhang, J.; Hong, F.W.; Xu, F.; Wang, L.P.; Zhao, F. Experimental study on the transient flow field near the free surface of the object exiting water. *J. Ship Mech.* **2002**, *6*, 45–50.
78. Wang, Y.; Chen, B.; Shi, H.; Jia, H.; Zhou, S.; Zhou, Y. Study on Supercavitation Inclined Water Outflow Process with First-Stage Light Gas Gun. In Proceedings of the 16th National Conference on Shock Waves and Shock Tubes, Atlanta, GA, USA, 16–20 June 2014; pp. 553–561.

79. Shi, H.; Chen, B.; Wang, Y. Experimental and numerical study of oblique water exit in free surface penetration by a blunt body's supercavity. *J. Exp. Fluid Mech.* **2016**, *30*, 29–35.
80. Wu, Q.G.; Ni, B.Y.; Bai, X.L.; Cui, B.; Sun, S.L. Experimental study on large deformation of free surface during water exit of a sphere. *Ocean Eng.* **2017**, *140*, 369–376. [[CrossRef](#)]
81. Baarholm, R.; Faltinsen, O.M. Wave impact underneath horizontal decks. *J. Mar. Sci. Technol.* **2004**, *9*, 1–13. [[CrossRef](#)]
82. Sun, L.; Sun, C.; Zhao, J. System design on small-scale solid of revolution exiting water test of scaled missiles. *Transducer Microsyst. Technol.* **2014**, *33*, 76–79.
83. Tveitnes, T.; Fairlie-Clarke, A.C.; Varyani, K. An experimental investigation into the constant velocity water entry of wedge-shaped sections. *Ocean Eng.* **2008**, *35*, 1463–1478. [[CrossRef](#)]
84. Lighthill, M.J. Drift. *J. Fluid Mech.* **1955**, *1*, 31–53. [[CrossRef](#)]
85. Faltinsen, O.; Kjærland, O.; Nøttveit, A.; Vinje, T. Water Impact Loads And Dynamic Response Of Horizontal Circular Cylinders In Offshore Structures. In Proceedings of the Offshore Technology Conference, Houston, TX, USA, 1–4 May 1977.
86. Peregrine, D.H. A Line Source Beneath a Free Surface. 1972. Available online: https://www.zhangqiaokeyan.com/ntis-science-report_other_thesis/020711919604.html (accessed on 19 September 2024).
87. Broeck, J.M.V.; Schwartz, L.W.; Tuck, E.O. Divergent Low-Froude-Number Series Expansion of Nonlinear FreeSurface Flow Problems. *Proc. R. Soc. A* **1978**, *361*, 207–224.
88. Breton, T.; Tassin, A.; Jacques, N. Experimental investigation of the water entry and/or exit of axisymmetric bodies. *J. Fluid Mech.* **2020**, *901*, A37. [[CrossRef](#)]
89. Tassin, A.; Jacques, N.; Alaoui, A.E.M.; Nème, A.; Leblé, B. Hydrodynamic loads during water impact of three-dimensional solids: Modelling and experiments. *J. Fluids Struct.* **2012**, *28*, 211–231. [[CrossRef](#)]
90. Ren, Z.Y.; Sun, L.Q.; Li, Z.P.; Xiao, W. Experimental Study on the Cavitation Development and Collapse Characteristics of Underwater Vehicle. *Astronaut. Syst. Eng. Technol.* **2021**, *5*, 42–49.
91. Logvinovich, G.V. *Hydrodynamics of Free-Boundary Flow*; Shanghai Jiao Tong University Press: Shanghai, China, 2012.
92. Reichardt, H.; Munzner, H. Rotationally symmetric source-sink bodies with predominantly constant pressure distributions. *Arm. Res. Est. Trans.* **1950**, *50*, 1–7.
93. Shi, H.H.; Zhou, D.H.; Lu, L.W.; Zhou, D.; Liu, Y. On the water exit of supercavitating projectiles with different head shapes. *Shock Waves* **2021**, *31*, 597–607. [[CrossRef](#)]
94. Albert, M. *Water Entry and the Cavity-Running Behavior of Missiles*; NASA STI/Recon Technical Report N 76; NASA: Washington, DC, USA, 1975.
95. Lu, J.; Wang, C.; Wei, Y.; Xu, H.; Song, W. Experimental Research on Cavity Evolution Pattern and Trajectory Characteristics in the Water-exit Process of Salvoed Revolving Bodies. *Acta Armamentarii* **2019**, *40*, 1226–1234.
96. Chen, Y.; Gong, Z.; Li, J.; Chen, X.; Lu, C. Numerical Investigation on the Regime of Cavitation Shedding and Collapse During the Water-Exit of Submerged Projectile. *J. Fluids Eng. Trans. ASME* **2020**, *142*, 142. [[CrossRef](#)]
97. Feng, Y.Y.; Zheng, Z.; Liu, H.P.; Zhou, Y. Effect of exit geometry of blowing air on friction drag of an underwater plate. *Ocean Eng.* **2022**, *257*. [[CrossRef](#)]
98. Qin, N.; Lu, C.; Li, J. Numerical Investigation of Characteristics of Water-Exit Ventilated Cavity Collapse. *J. Shanghai Jiao Tong Univ.* **2016**, *21*, 530–540. [[CrossRef](#)]
99. Guo, Z.; Zhao, Y.; Zhang, X.; Lyu, X. On the cavity flow of a cylinder exiting water obliquely. *Ocean Eng.* **2023**, *281*, 114683. [[CrossRef](#)]
100. Nguyen, V.T.; Phan, T.H.; Duy, T.N.; Park, W.G. Unsteady cavitation around submerged and water-exit projectiles under the effect of the free surface: A numerical study. *Ocean Eng.* **2022**, *263*, 112368. [[CrossRef](#)]
101. Zhang, G.; You, C.; Wei, H.; Sun, T.; Yang, B. Experimental study on the effects of brash ice on the water-exit dynamics of an underwater vehicle. *Appl. Ocean Res.* **2021**, *117*, 102948. [[CrossRef](#)]
102. Zhang, Y.; Wang, W.; Zhang, F.; Zhang, J.; Chen, C.; Deng, Y.; A, R. Study on the Effect of Bubble Sizes and Gas Nuclei Number on Incipient Cavitation. *Yellow River* **2013**, *35*, 4.
103. Knapp, R.T.; Daily, J.W.; Hammit, F.G. *Cavitation*; McGraw Hill Book CO: New York, NY, USA, 1970.
104. Harvey, E.N.; Whiteley, A.H.; Mcelroy, W.D.; Pease, D.C.; Barnes, D.K. Bubble formation in animals. II. Gas nuclei and their distribution in blood and tissues. *J. Cell. Comp. Physiol.* **1944**, *24*, 23–34. [[CrossRef](#)]
105. Hervey, E.N.; Barnes, D.K.; Mcelroy, W.D.; Whiteley, A.H.; Pease, D.C. Removal of Gas Nuclei from Liquids and Surfaces. *J. Am. Chem. Soc.* **2002**, *67*, 156–157. [[CrossRef](#)]
106. Harvey, E.N.; Mcelroy, W.D.; Whiteley, A.H. On Cavity Formation in Water. *J. Appl. Phys.* **1947**, *18*, 162–172. [[CrossRef](#)]
107. Luo, X.; Ji, B.; Peng, X.; Liu, D. *Basic Theory and Application of Cavitation*; Tsinghua University Press: Beijing, China, 2020.
108. Ackeret, J. Experimentelle und theoretische untersuchungen uberhohlraumbildung (kavitation) im wasser. *Tech. Mech. Thermodyn.* **1930**, *1*, 1–2.
109. Yang, Z. Discussion and new checking of scale effects for cavitation inception. *Chin. J. Hydrodyn.* **2008**, *23*, 5.
110. Holl, J.W.; Treaster, A. Cavitation Hysteresis. *Basic Eng.* **1966**, *88*, 199–211. [[CrossRef](#)]
111. Meulen, J.H.J.V.D. Cavitation on hemispherical nosed teflon bodies. *Int. Shipbuild. Prog.* **1972**, *19*, 333–341. [[CrossRef](#)]
112. Pan, S. *The Encyclopedia of China: Mechanics Volume*; China Encyclopedia Publishing House: Beijing, China, 1985.

113. Self, M.; Ripken, J.F. *Steady-State Cavity Studies in a Free-Jet Water Tunnel*; St. Anthony Falls Hydraulic Laboratory: Minneapolis, MN, USA, 1955.
114. Haohao, H.; Yanping, S.; Jianyang, Y.; Fu, C.; Tian, L. Numerical analysis of water exit for a sphere with constant velocity using the lattice Boltzmann method. *Appl. Ocean Res.* **2019**, *84*, 163–178. [[CrossRef](#)]
115. Zhang, X.Y.; Lyu, X.J.; Fan, X.D. Numerical Study on the Vertical Water Exit of A Cylinder with Cavity. *China Ocean Eng.* **2022**, *36*, 734–742. [[CrossRef](#)]
116. Zhang, Y.; Duan, W.; Ma, S.; Liao, K. Numerical Simulation of Water Entry and Exit Problems by an Adaptive Cartesian Grid Method. *Int. J. Offshore Polar Eng.* **2022**, *32*, 66–73. [[CrossRef](#)]
117. Moran, J. *On the Hydrodynamic Theory of Water-Exit and -Entry*; Therm Advanced Research Inc.: Ithaca, NY, USA, 1965.
118. Zhang, C.; Zhu, Y.; Hu, X. An efficient multi-resolution SPH framework for multi-phase fluid-structure interactions. *Sci. China Phys.* **2023**, *66*, 92–113. [[CrossRef](#)]
119. Longuet-Higgins, M.S.; Cokelet, E.D. The Deformation of Steep Surface Waves on Water. I. A Numerical Method of Computation. *Proc. R. Soc. A Math. Phys. Eng. Sci.* **1976**, *350*, 1–26.
120. Ye, Q.; He, Y. Nonlinear Numerical Solution for Vertical Water Exit of Axisymmetric Body. *J. Appl. Mech.* **1986**, *3*, 25–30.
121. Zhu, X.; Faltinsen, O.M.; Hu, C. Water Entry and Exit of a Horizontal Circular Cylinder. *J. Offshore Mech. Arct. Eng.* **2006**, *129*, 253–264. [[CrossRef](#)]
122. Tyvand, P.A.; Miloh, T. Free-surface flow due to impulsive motion of a submerged circular cylinder. *J. Fluid Mech.* **1995**, *286*, 67–101. [[CrossRef](#)]
123. Rajavaheinthan, R.; Greenhow, M. Constant acceleration exit of two-dimensional free-surface-piercing bodies. *Appl. Ocean Res.* **2015**, *50*, 30–46. [[CrossRef](#)]
124. Sun, S.L.; Wu, G.X. Oblique water entry of a cone by a fully three-dimensional nonlinear method. *J. Fluids Struct.* **2013**, *42*, 313–332. [[CrossRef](#)]
125. Wu, G.X. Two-dimensional liquid column and liquid droplet impact on a solid wedge. *Q. J. Mech. Appl. Math.* **2007**, *60*, 497–511. [[CrossRef](#)]
126. Ma, Z.; Hu, J.; Feng, J.; Liu, A.; Chen, G. A longitudinal air–water trans-media dynamic model for slender vehicles under low-speed condition. *Nonlinear Dyn.* **2020**, *99*, 1195–1210. [[CrossRef](#)]
127. Chen, Y.; Li, J.; Gong, Z.; Chen, X.; Lu, C. LES investigation on cavitating flow structures and loads of water-exiting submerged vehicles using a uniform filter of octree-based grids. *Ocean Eng.* **2021**, *225*, 108811. [[CrossRef](#)]
128. Liu, Z.; Yi, S.; Yan, K.; Xu, S.; Wang, B. Numerical Simulation Of Water-exit Cavity. In Proceedings of the Fifth International Symposium on Cavitation (CAV2003), Osaka, Japan, 1–4 November 2003.
129. Chu, X.S.; Yan, K.; Wang, Z.; Zhang, K.; Feng, G.; Chen, W.Q. Numerical simulation of water-exit of a cylinder with cavities. *J. Hydrodyn. Ser. B* **2010**, *22*, 877–881. [[CrossRef](#)]
130. Saghatchi, R.; Ghazanfarian, J.; Gorji-Bandpy, M. Turbulent fluid-structure interaction of water-entry/exit of a rotating circular cylinder using SPH method. *Int. J. Mod. Phys. C* **2015**, *26*, 1550088.
131. Wu Y; Cai X; He M; Zhang J. Numerical Research of Water-exit of Slender Body Based on SPH Method. In Proceedings of the 11th National Fluid Mechanics Conference, Shenzhen, China, 3–7 December 2020.
132. Bašić, J.; Degiuli, N.; Werner, A. Simulation of Water Entry and Exit of a Circular Cylinder Using the ISPH Method. *Trans. FAMENA* **2014**, *38*, 45–62.
133. Hu, S.; Lu, C. Numerical Study on Water-exit of Elastic Body at High Speed. In Proceedings of the 14th National Hydrodynamics Conference, Changchun, China, 8–13 August 2017; pp. 914–920.

Disclaimer/Publisher’s Note: The statements, opinions and data contained in all publications are solely those of the individual author(s) and contributor(s) and not of MDPI and/or the editor(s). MDPI and/or the editor(s) disclaim responsibility for any injury to people or property resulting from any ideas, methods, instructions or products referred to in the content.